ISSN 0016-7932, Geomagnetism and Aeronomy, 2014, Vol. 54, No. 4, pp. 406–415. © Pleiades Publishing, Ltd., 2014.
Original Russian Text © G.P. Chernov, V.V. Fomichev, R.V. Gorgutsa, A.K. Markeev, D.E. Sobolev, A. Hillaris, K. Alissandrakis, 2014, published in Geomagnetizm i Aeronomiya, 2014, Vol. 54, No. 4, pp. 444–454.

Fine Structural Features of Radio-Frequency Radiation of the Solar Flare of February 12, 2010

G. P. Chernov[a], V. V. Fomichev[a], R. V. Gorgutsa[a], A. K. Markeev[a], D. E. Sobolev[a], A. Hillaris[b], K. Alissandrakis[c]

[a] *Pushkov Institute of Terrestrial Magnetism, Ionosphere, and Radio Wave Propagation, Russian Academy of Sciences (IZMIRAN), Kaluzhskoe shosse 4, Troitsk, Moscow oblast, 142190 Russia*

[b] *Section of Astro-Geophysics, Department of Physics, University of Ioannina, 45110 Ioannina, Greece*

[c] *Section of Astrophysics, Astronomy and Mechanics, Department of Physics, University of Athens, Panepistimiopolis 15784, Zografos, Greece*

e-mail: gchernov@izmiran.rssi.ru

Received July 30, 2013; in final form, February 9, 2014

Abstract—Solar radio emission records received at the IZMIRAN spectrograph (25–270 MHz) during the solar flare event of February 12, 2010 are analyzed. Different fine structures were observed in three large groups of type III bursts against a low continuum. According to data from the Nancay radioheliograph, sources of all three groups of bursts were located in one active region, 11046, and their emissions were accompanied by soft X-ray bursts (GOES satellite): C7.9 at 0721 UT, B9.6 at 0940 UT, and M8.3 at 1125 UT. After the first group of bursts, classical fiber bursts were observed in combination with reverse-drift fiber bursts with unusual arc drift. After the third (the most powerful) group, stable second-length pulsations and slow-drift fiber bursts were observed, the instantaneous frequency bands of which were an order of magnitude larger than the frequency band of classical fiber bursts, and the frequency drift was several times lower. More complex fiber bursts were observed in the weakest group in the time range 0940:39–0942:00 UT. They were narrow-band (~0.5 MHz) fiber bursts, periodically recurring in a narrow frequency band (5–6 MHz) during several seconds. The presence of many chaotically drifting ensembles of fibers, crossing and superimposing on one another, is a feature of this event. It is assumed that occurrence of these structures can be connected with the existence of many small shock fronts behind the leading edge of a coronal mass ejection.

DOI: 10.1134/S0016793214040021

1. INTRODUCTIONS

Stripes in emission and absorption in the form of regular zebra structures or intermediate drift bursts (IDB), or fiber bursts, against continuum radiation of type IV radio bursts in the meter and decimeter wave ranges have been studied for a long time and classified in monographs (see, e.g., (Kruger, 1983)) and reviews (Slottje, 1981; Chernov, 2006, 2011). Ensembles of twisted narrow-band fibers are among such structures in the VHF range; their nature remains understudied. They were first recorded on the IZMIRAN spectrograph during the event of January 24, 1985 and discussed in the works (Aurass et al., 1987; Mann et al., 1989). The main properties of such fiber ensembles are that they are sets of periodic fibers in the 2–3 MHz band with arbitrary oscillating frequency drifts and absorption at the low-frequency edge (Chernov, 2008). Narrow bands usually follow with overlapping in frequency, and the rate of recurrence is 2–3 times higher than that of IDB (Chernov, 1997). The general form of these periodic fiber bursts is similar to a rope of fibers in the dynamic spectrum; therefore, hereinafter we use this term.

An opinion was accepted after the first publications (Aurass et al., 1987; Mann et al., 1989) that fiber ropes are quite seldom phenomena observed during the post-flash phase of large bursts and accompanying zebra structures. However, a careful analysis of observation data has shown that fiber ropes are quite frequent in a wide meter wave range, not only as parts of developed zebra structures but also as isolated bursts during the pulse phase after type III bursts and before type II bursts. Comparison of the dynamic spectra of such fiber ropes (on one time scale) received at Tremsdorf station and IZMIRAN has shown an exact correspondence of fibers (Chernov, 2008).

An analysis of observations at lower frequencies (20–40 MHz) carried out by Chernov in 2004 and in 2006 in more detail (Chernov, 2004, 2006) showed that ropes of strictly periodic fibers were observed between two type II bursts, and their radio emission should be from an altitude range between two shock fronts propagating with different velocities. Different fiber ropes without noticeable LF-absorption were observed at frequencies of 19–29 MHz in the form of a fine structure of complex type II bursts (Chernov et al., 2007). Such ropes occurred at the instant when a shock wave

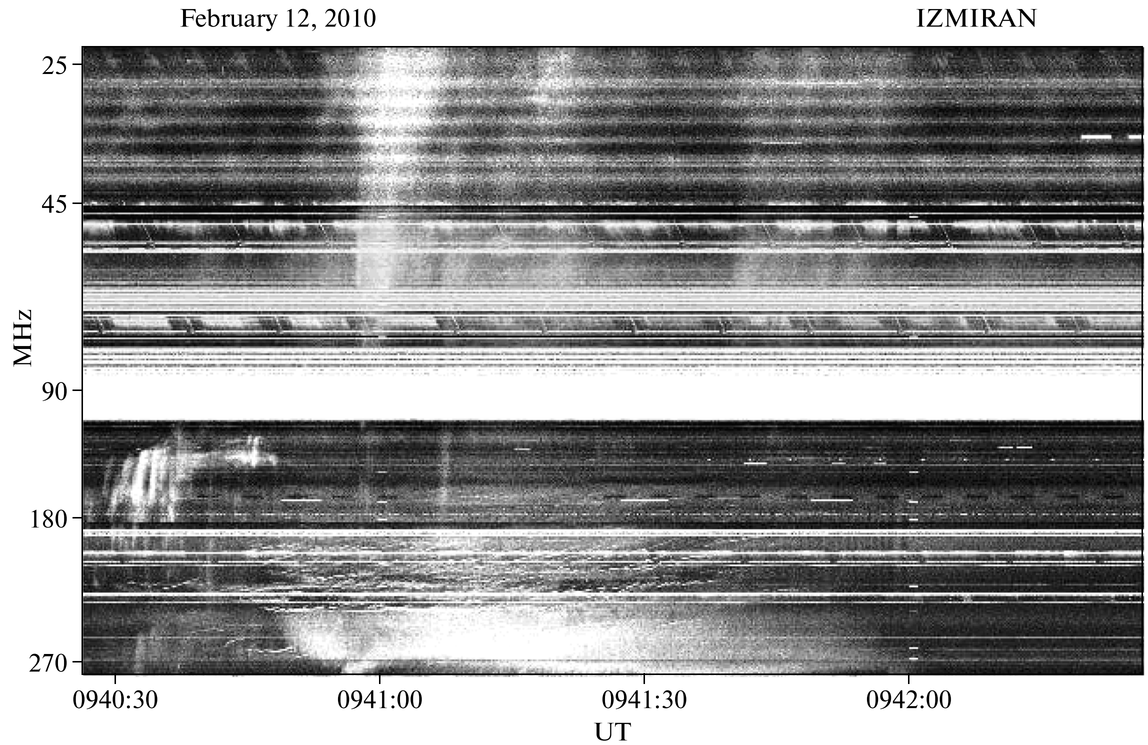

Fig. 1. General view of the radio radiation spectrum measured on the IZMIRAN spectrograph in the 25–270 MHz range after 0940 UT. Chaotic fiber ropes appeared against a continuum (probably of type V) in the 170–270 MHz range after a group of type III bursts in a restricted frequency range. Type III bursts continued at lower frequencies; their initial frequencies touched the LF continuum boundary.

caught up with a coronal mass ejection (CME), i.e., the radio emission came from a region between the leading edge of CME and a trail shock wave.

The purpose of this work is to reveal new features of these structures on the basis of IZMIRAN spectrograph observations (25–270 MHz) of the event of February 12, 2010 in comparison with earlier observed events.

2. NEW OBSERVATIONS

Three groups of type III bursts were observed on February 12, 2010; they were accompanied by soft X-ray bursts (GOES): C7.9 at 0721 UT, B9.6 at 0940 UT, and M8.3 at 1125 UT. All the three groups came from one active region, 11046, but the corresponding Hα flares occurred in different regions: in N24E13 at 0721, in N22T07 at 0940, and in N26E11 at 1126. According to the Nancay spectropolarimeter data, three groups of type III bursts were right-hand polarized in the 20–70 MHz range. Hence, one may assume that the south-seeking magnetic polarity of the leading sunspot predominated high in the corona; therefore, the emission corresponded to the ordinary mode. Each group was accompanied by the type V continuum radiation, and two type II bursts were observed after the third group.

An unusual fine structure, different in each case, was observed in the continuum radiation, which answers the assumption that radio sources of the continuum were in different magnetic loops.

2.1. Bursts at 0940 UT

Numerous fiber ropes occurred in the weakest burst at 0940 UT in the 180–270 MHz frequency range (Fig. 1). The ropes were observed simultaneously with several groups of type III bursts, which were typical for other events with fiber ropes (Chernov, 2008). All fiber ropes were observed against type V continuum radiation. During that event, we observed many chaotically drifting ropes, which intersected and superimposed on one another. Up to ten different ropes were distinguishable simultaneously in the 185–225 MHz frequency band. Moreover, in contrast to the previous data, the fibers did not repeat in each rope but followed almost chaotically in frequency and time. Figure 2 shows magnified segments of fiber ropes received simultaneously at IZMIRAN and the Greek spectrograph ARTEMIS-IV (Kontogeorgos et al., 2006). All of the main elements of the fine structure coincide in both spectra in time and frequency, which confirms their solar origin.

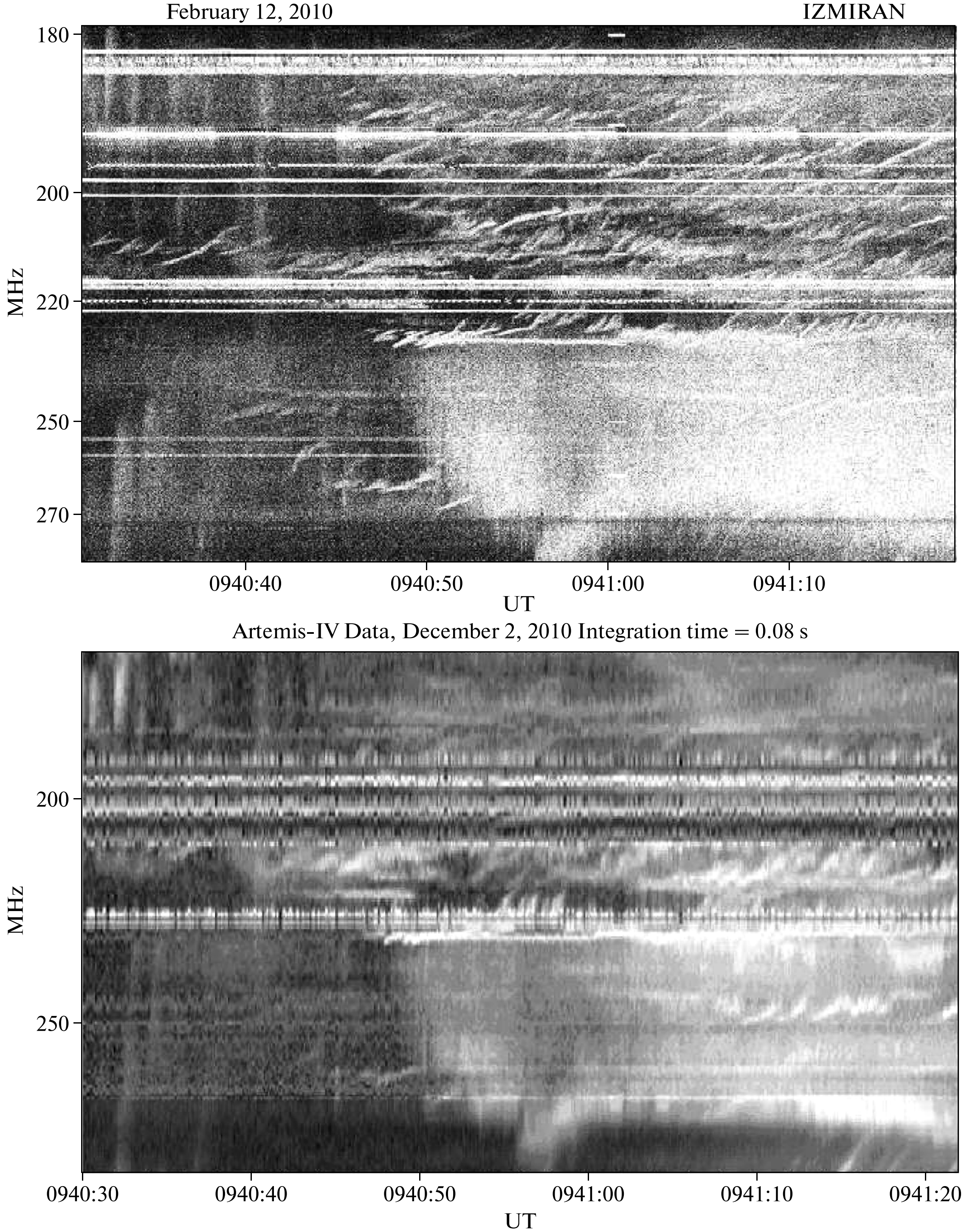

Fig. 2. Segments of dynamics spectra with fiber ropes in the 180–280 MHz range measured simultaneously on IZMIRAN and ARTEMIS-IV (Greece) spectrographs.

A family of fiber ropes forms a braided (by Slottje (1981)) zebra structure.

An instantaneous width of the frequency band of each rope does not exceed 1 MHz. All small fibers drift to low frequencies, but the drift velocity varies from one fiber to another, and even individual fibers have an arc form. The length of each fiber also varies from 1 s (and shorter) in the spectrum head (Fig. 2) to 5–7 s in its end. The frequency drift of individual fibers (≈–2 MHz s^{-1}) and ropes in total (≈–0.5 MHz s^{-1}) becomes more sta-

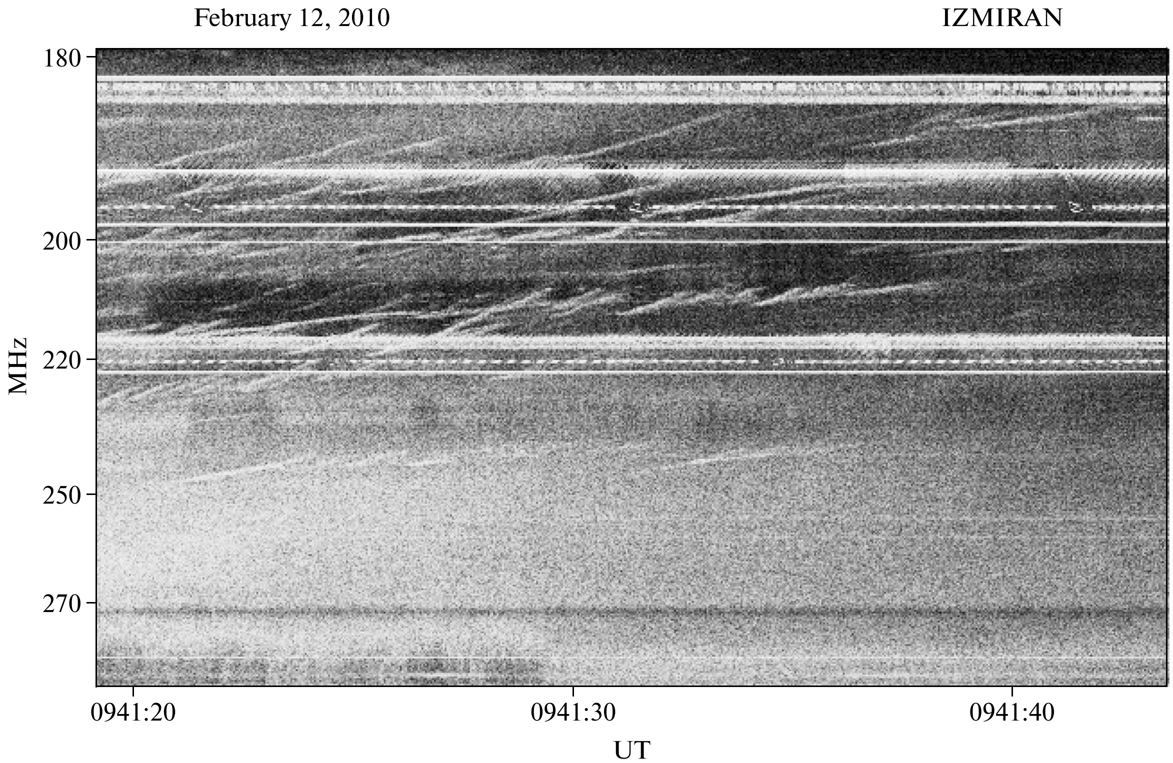

Fig. 3. Positions of fiber ropes. Frequency drift of the ropes and individual fibers is more stable.

ble toward the end of the segment (Fig. 3). Here, they are close in parameters to fiber ropes discussed earlier (Chernov, 1997, 2006).

Fiber ropes were sometimes crossed by individual fibers (0940:50 and 0941:25 UT), which could be evidence of spaced radio sources at close altitudes in the corona.

Fiber ropes are seen against a flare continuum existing along with them (see, e.g., 0941:10 UT at frequencies close to 235 MHz in Figs. 2 and 3). According to data from the Zürich spectrograph (st. Bleien) in the 100–800 MHz range, this continuum (speckled with fast pulsations) continued until frequencies of about 800 MHz, and according to Ondrejov observatory spectrograph data, even higher than 2 GHz. The radio flux at 3 GHz was 200 s.f.u. (1 s.f.u. = 10^{-22} W m^{-2} Hz^{-1}); however, the radio radiation maximum was in the meter range, ~16000 s.f.u. at 245 MHz.

2.2. Bursts after 1125 UT

This group of bursts was the most powerful in the day (the X-ray flare importance was M9.3). It consisted of two phases; each of them included type II bursts (Fig. 4). The first phase, at 1125–1128 UT, was more powerful; the hard X-ray maximum fell in this interval. During the second stage, at 1129–1133 UT, the group of type III bursts was weaker and was accompanied by a soft X-ray burst, though the type II burst was stronger there than during the first phase. However, according to the analysis of optical and X-ray data (Alissandrakis et al., 2011), a strong CME was recorded on pictures in the 195 Å band (STEREO satellite behind) and in the Hα line (Catania obs.) just before the first type II burst at 1125 UT, while only coronal beam deflection during the expansion of a spherical ejection (called the second disturbance) was noted before the second type II burst.

No continuum radiation (type V) was observed after the first group of strong type III bursts with the first weak type II burst at the end. This means the absence of a trap for particles and departure of the shock front high into the corona.

The second type II burst started about 10 minutes after the beginning of the second group of type III bursts (the second phase of the event); it was observed against a low continuum (Fig. 4). The continuum in the 200–400 MHz frequency range was modulated by fast pulsations; the absorption pulsations (sudden reductions type) predominated first and then they transformed into the radiation pulsations after 1130:00 UT, which is better seen in the magnified fragment in Fig. 5. The pulsations cover both the baseband A of the second type II burst and two unusual (narrow) bands designated as B1 and B2 in Fig. 4. This can occur if the sources of the pulsations, continuum, and type II burst coincided at that instant. All the pulsations had negative frequency drift ~–50 MHz s^{-1}. The zigzag band A

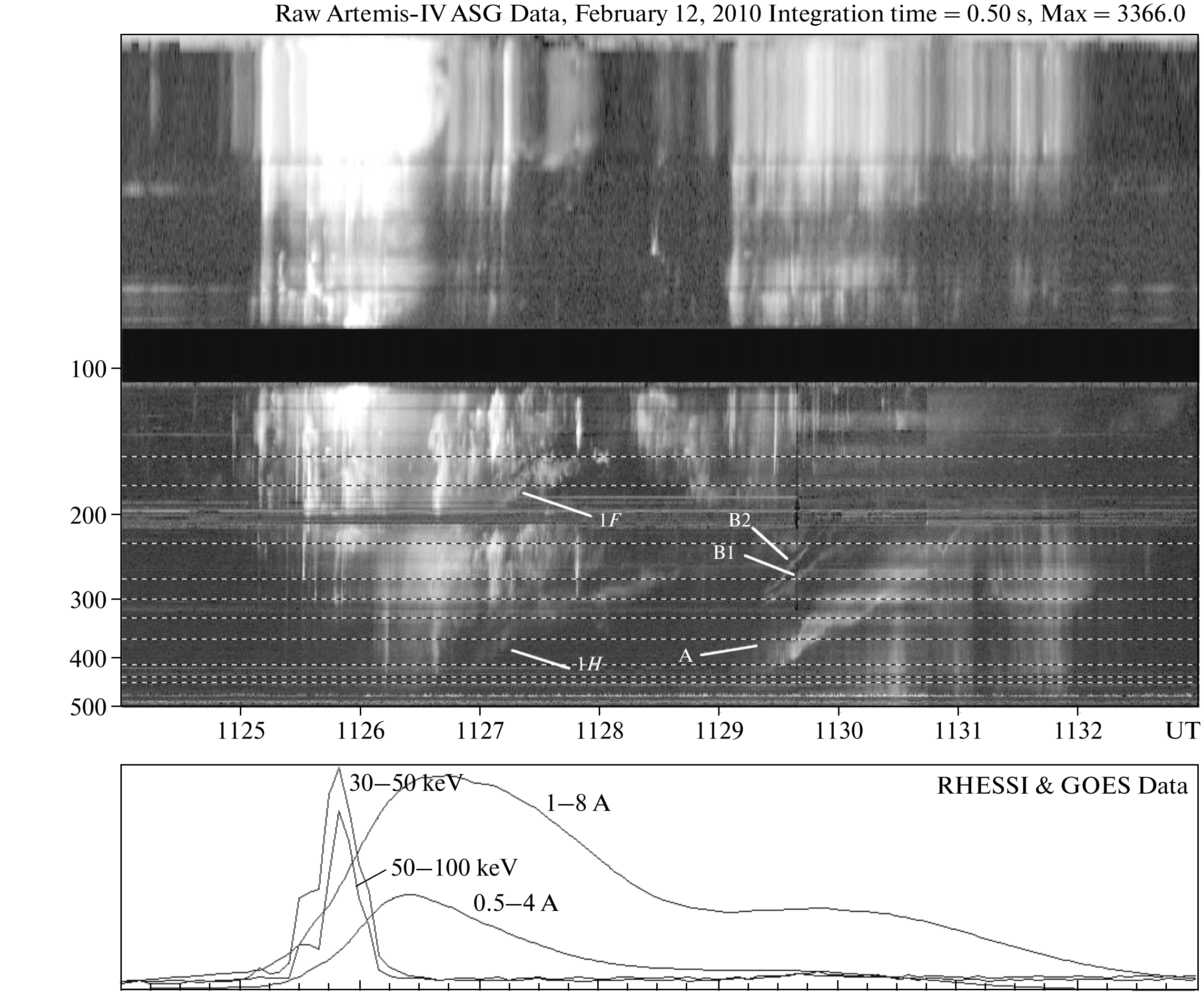

Fig. 4. Dynamic spectrum of the third group of type III bursts according to ARTEMIS-IV data in the 25–500 MHz range, which shows the presence of two type II bursts. Horizontal dashed lines corresponds to frequencies of the Nancay radioheliograph; 1*F* and 1*H* designate the base frequency and the second harmonics of the first type II burst; A, B1, and B2 show the baseband of the second type II burst and two fine-structure bands. Time profiles of the intensities of soft and hard X-ray radiation by GOES and RHESSI data are shown in the bottom.

ends at frequencies <240 MHz with a V-type burst (Fig. 6) with explicit absorption of the continuum at its HF edge, which makes it similar to the B1 and B2 bands. Simultaneously, the pulsations change the frequency drift to positive and slower ~25 MHz s^{-1} (Fig. 6).

2.3. The First Group of Bursts at 0721 UT

The flare at 0721 UT was of medium power (C7.9/1N), but a group of type III bursts was the most numerous, more than 30 bursts for three minutes in the 0721–0724 UT range (Fig. 7). The radiation maximum was in the meter and decimeter ranges. A weak continuum (type V burst) was observed at frequencies close to the initial frequencies of type III bursts and higher. Two groups of unusual fast-drift fibers (bottom spectrum in Fig. 7) appeared against this continuum: fibers before 0724 UT (similar to fiber bursts) drifted to low frequencies, and those after drifted to high frequencies.

Fibers do not show arc drift close to 0725:00 UT. Several bands similar to a weak zebra structure are distinguishable, but no fiber ropes were observed.

It is interesting to compare the positions of sources of radio radiation of different fine structure in three flares of February 12, 2010 in the AR. According to data from the X-ray telescope Hinode XRT, bright X-ray loops remained quite stable during the day. Positions of the flares (*1*, *2*, and *3* according to the time of occurrence) are shown in the X-ray image of AR 11046 (Fig. 8).

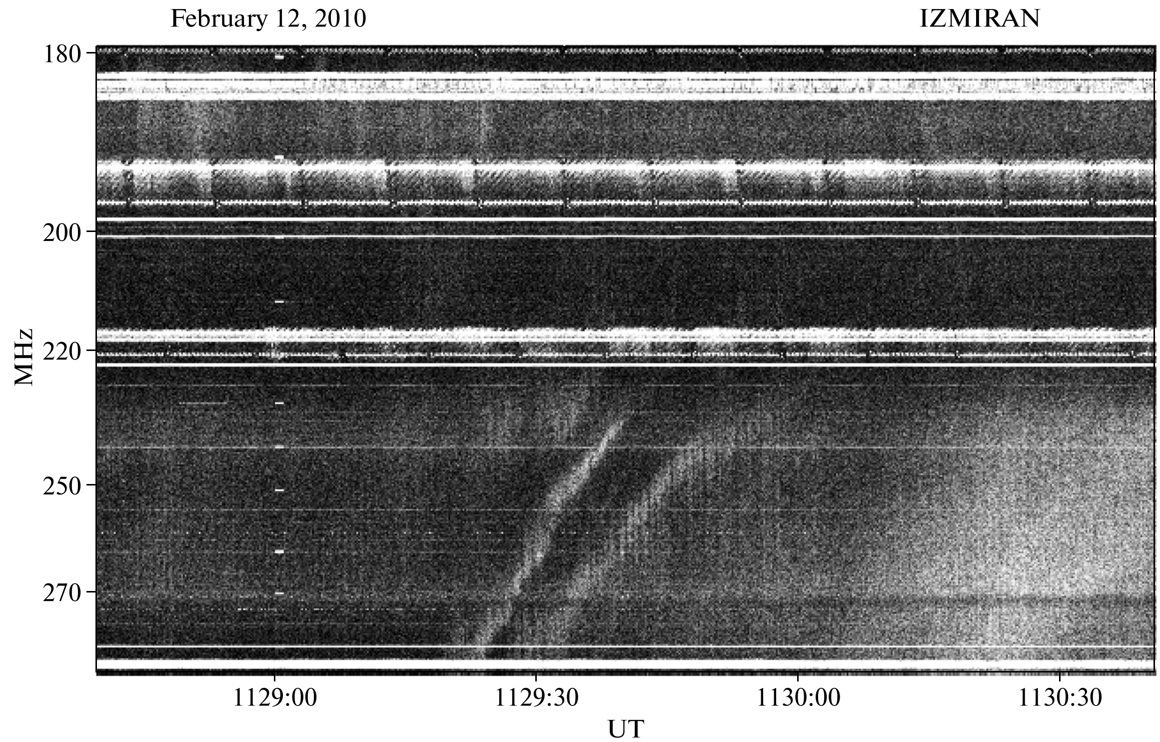

Fig. 5. Magnified fragment of slow-drift bands, which can be taken for split bands of the second type II burst. The spectrum is complicated by the continuum radiation with fast pulsations of ~0.7 in period.

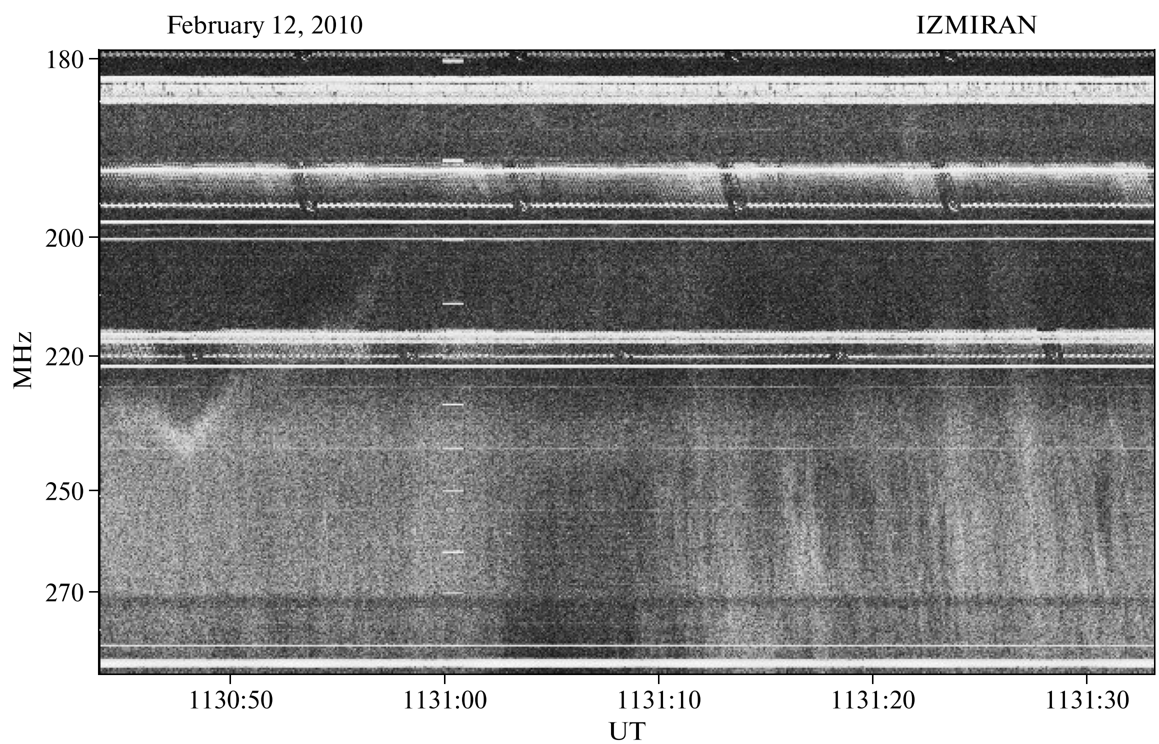

Fig. 6. Continuation of a fine structure after the second type II burst. The zigzag burst with LF absorption exactly coincides with the ARTEMIS-IV spectrum.

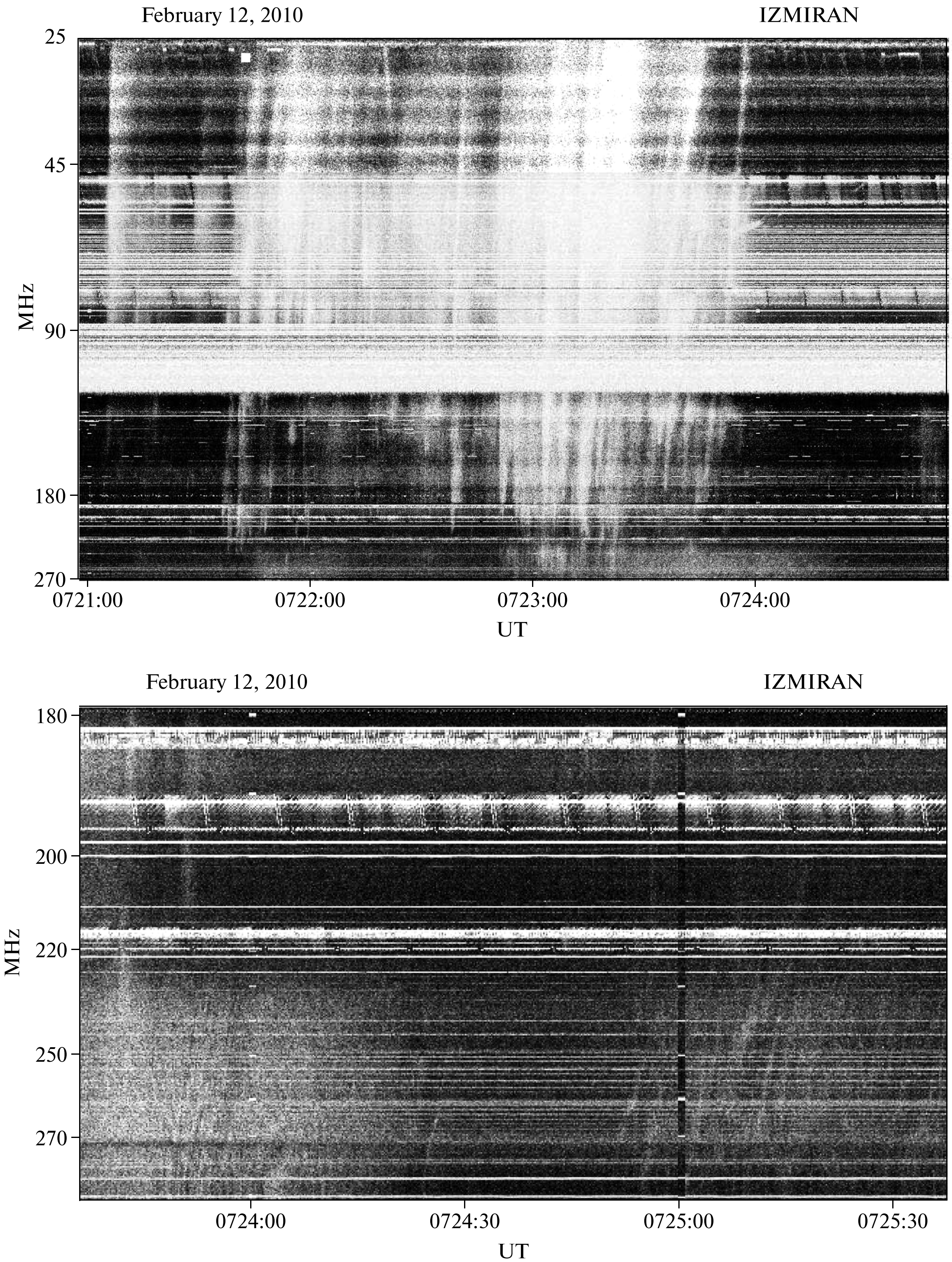

Fig. 7. General view of the IZMIRAN spectrum in the 25–270 MHz range after the first group of type III bursts at 0721 UT (upper spectrum). The following fine structure in the form of irregular fiber bursts in the 210–270 MHz range (bottom spectrum).

The first flare (at 0721 UT) was between the bases of large, bright X-ray loops that formed a shear in the north-western (N-W) part of the AR between the upper N-W loop and the bottom east-western (E-W) loop, with weak brightening of the flare at the point of their approach. It is natural to assume that this flare loops (with the shear) continued high into the corona in the form of successive magnetic loops. The radio

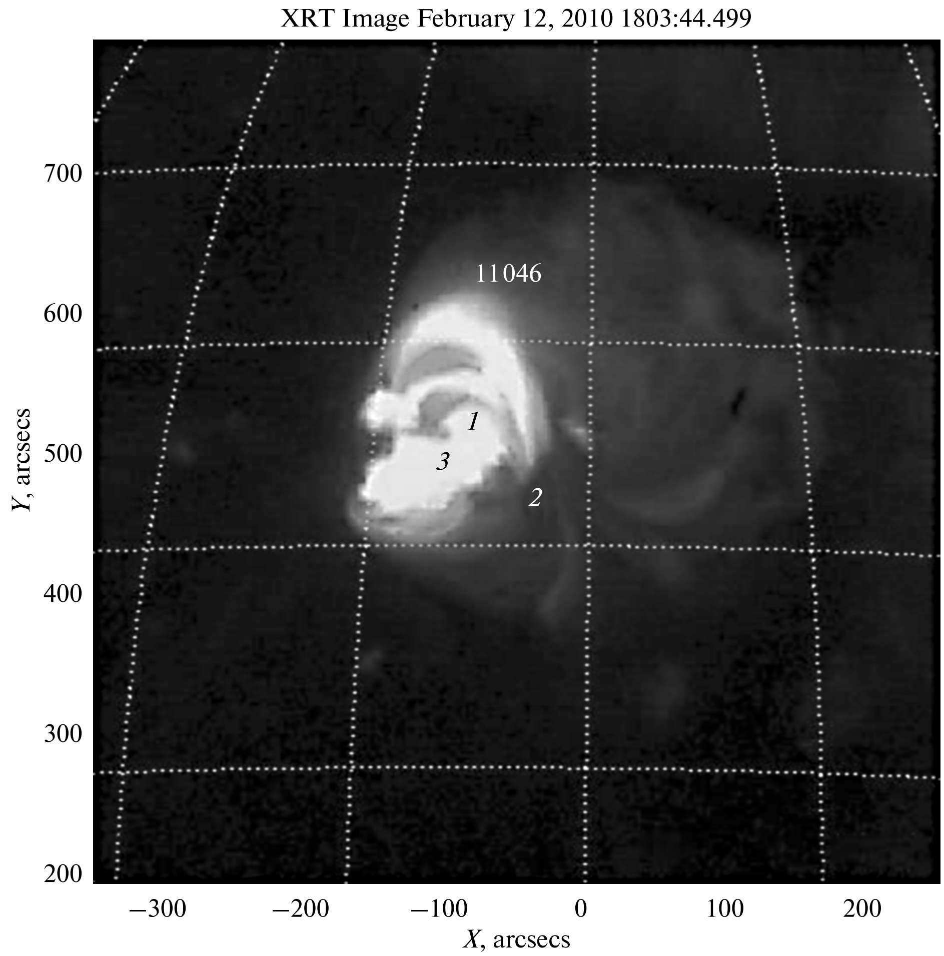

Fig. 8. Hinode XRT image of active region 11046 in soft X-rays; *1*, *2*, and *3* show approximate positions of three flare centers on February 12, 2010 in the AR.

radiation maximum of the first event fell into the meter range; therefore, one may assume that the acceleration of particles occurred high in the corona. A strong group of type III bursts testifies to the open structure of the magnetic field above the acceleration region. Downward-accelerated particles were partly captured in the closed magnetic trap, which resulted in a type V continuum burst. A change in sign of the frequency drift of fibers around 0724 UT from negative to positive pointed to a possible reflection of particles at the bottom of the trap and their following propagation along the loop with some radiation attenuation at the instant of change in the drift sign (at the top of the loop).

The second flare occurred in the western foot of the large N-W loop. The radiation maximum was in the meter range; therefore, particle acceleration occurred still higher in the corona. Particles were captured in the western foot of the large N-W loop (the probable source of type V continuum). No explicit type II burst was observed at 0940 UT, though the fact that the shock wave could accompany the CME could not be excluded.

Different scenarios of flares help to explain the data on CME obtained from STEREO satellite coronagraphs. Figure 8 shows CME pictures obtained at the COR2 coronagraph (behind) after the second (left side) and the third flares (right side). The northern base of the loop-type CME at 1024 UT shows inhomogeneities in the form of cross-concentric bands (clearly seen in magnified images). They begin directly at the release of CME after a screen at altitudes $2R_S$. If the velocity of CME is considered equal to about 650 km/s, then these inhomogeneities turn out to be at altitudes of the meter range (plasma frequency) at about 0940 UT. Thus, the tail of the CME had to cross the large loop just at the instant of occurrence of fiber ropes. Positions of radio sources of the first $1F$ and the second $1H$ (Fig. 4) harmonics almost coincided in Nancay radioheliograms at several frequencies (Alissandrakis et al., 2011). Sources of both bursts revealed upward motion with time (propagation of shock fronts).

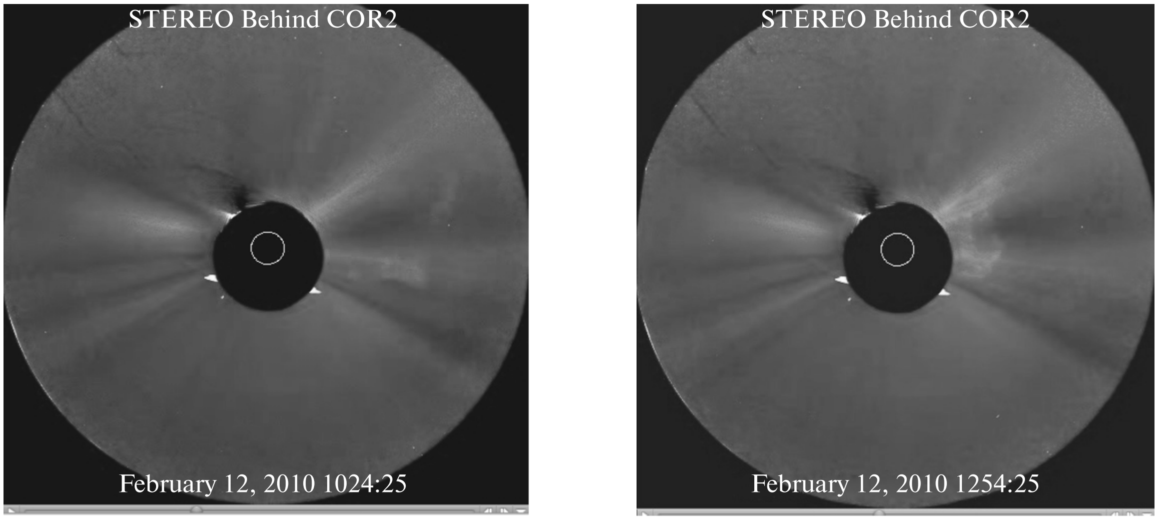

Fig. 9. Images of two CMEs obtained during the STEREO behind COR2 experiment at 1024:25 and 1254:25 UT, the beginning of which almost coincides with appearance of fiber ropes at 0940 UT and unusual slow-drift bands.

The third flare occurred in the eastern part of the AR. The right part of Fig. 9 shows that the leading front of the CME propagated to about 5 R_S at 1254 UT. Alissandrakis et al. (2011) showed that the leading edge of the CME appeared in a STEREO COR1 image at 1135 UT at an altitude of $1R_S$; i.e., its velocity is ~750 km/s if we connect the CME start with the beginning of the flare. The second type II burst was connected with an additional disturbance that occurred at the instant of touchdown of the first spherical ejection with the large N-W loop (Alissandrakis et al., 2011). The first ejection occurred 3° to the east of the flare node in Hα (*3* in Fig. 8).

In this case, fast particles could be captured into the bottom E-W loop (source of type V continuum). Unusual B1 and B2 bands and zigzag band with LF absorption (Fig. 4) are probably connected with radiation from a strongly inhomogeneous source at the point of a shock front collision with the upper loop. The change in sign of the frequency drift of fast pulsations (Fig. 6) provides evidence of particle motion along the entire E-W loop.

The positions of sources of hard X-rays in the 25–50 keV energy range coincided with the corresponding flare positions (*1*, *2*, and *3*) in the Hα line, according to RHESSI data (Fig. 8), which supports the acceleration of fast particles during all the three events.

2.4. Conclusions from Observations

Fiber ropes form after groups of type III bursts unaccompanied by explicit type II bursts, not only in large radio bursts but also in relatively weak ones.

Comparison of the new and previous data shows that all fiber ropes are kindred phenomena and require a common approach to their interpretation. However, the fiber ropes at 0940–0942 UT differ in their chaotic character: they cross and superimpose on one another. Up to ten different ropes are distinguishable simultaneously in the 185–225 MHz frequency range. In addition, in contrast to the previous data, the fibers do not repeat in each rope but follow almost chaotically in frequency and time.

Analysis of previous events has shown that fiber ropes appear at the instant when a shock front catches up with a CME. A CME was also recorded in the event of February 12, 2010. In addition, the flare continuum in the 150–270 MHz range is probably a type V burst, which supports the existence of a magnetic trap high in the corona.

Fibers in ropes are often observed with overlapping in time and frequency, but sometimes (more often at the end of rope) they can follow with a time lag.

The fiber length and recurrence rate are rarely stable; they mainly increase from ~0.5 s in the beginning to several seconds at the end of a rope.

Part of the ropes and the fibers composing them reveals LF absorption. Thus, the fibers in the ropes are similar to ordinary bursts with intermediate drift (Kuijpers, 1975), but they drift in a narrow frequency band and repeat more often.

All three groups of type III bursts originated from one active region but from different parts. The appearance of fiber ropes at 0940:30 UT coincided with the instant when the CME crossed the large N-W flare loop. Numerous narrow inhomogeneities in the tail of the CME could be sources of the fiber ropes. Analysis of the scenarios of the flares at 0721 and 1125 UT shows a possible condition for the generation of fast pulsations and unusual fibers with LF absorption.

3. POSSIBLE MECHANISMS OF EMISSION

To analyze the event under study, we accept a more probable model of ropes of strictly periodic fibers with the capture of particles (accelerated in a shock front) into a small trap between the second shock front and the leading edge of the CME. This model proved to be correct by the coincidence of the rope appearance with the instant of intersection of the shock-front and CME trajectories in the altitude/time diagram for four events (Chernov, 2008). Within the model, existence of many small shock waves behind the leading edge of CME should be assumed. It is possible that such a turbulent zone could really exist in the CME tail, if proceeding from the strongly inhomogeneous structure in the CME pictures made in the STEREO experiment (STEREO behind COR2) at 1024:25 and 1254:25 UT (Fig. 9).

In addition, all fiber ropes were observed against type V continuum radiation, the source of which was, as is commonly accepted, a loop magnetic trap for fast particles. Moreover, they were mainly observed in the LF part of the continuum, i.e., the radiation came from the top of such a trap. The CME should pass through this top of the trap during the beginning stage. Just this can be a feature of the source of numerous fiber ropes. Particles captured in the trap earlier were additionally captured into inhomogeneities behind the leading edge of the CME. Thus, numerous fiber ropes reflect a complex structure of inhomogeneities in the CME in our case.

4. CONCLUSIONS

The main purpose of this work was to analyze causes of the appearance of complex ropes of radio fibers in a relatively weak event, while no ropes of fibers were observed in stronger events occurring in the same active region on the same day of February 12, 2010.

A feature of the event with complex ropes of fibers at frequencies of 180–270 MHz at 0940 UT was the coincidence of the instant of their appearance with the instant when the large flare loop (source of type V continuum radiation) crossed inhomogeneities behind the leading edge of CME. This was not observed during other two events, but the condition for the generation of another fine structure (fast pulsations and unusual fibers) was fulfilled during them.

Analysis of the main parameters of the fiber ropes has shown that they are kindred, with different fiber ropes observed earlier in other events, and require a common approach to their interpretation. The most probable cause of fiber radiation may be the generation of periodic fibers with intermediate frequency drift (fiber bursts) in small magnetic traps formed in the source between shock fronts and inhomogeneities behind the leading edge of a CME.

ACKNOWLEDGMENTS

The authors are grateful to A. Benz for provided spectra from st. Bleien. We are also grateful to the teams of SOHO, RHESSI, and STEREO experiment for free access to the databases. The work was financially supported by the Russian Foundation for Basic Research (grant no. 14-02-00367).

REFERENCES

Alissandrakis, C.E., Nindos, A., Patsourakos, S., and Hillaris, A., and the ARTEMIS group, Multi-wavelength observations of a metric type II event, *Report in EPSM-13 Conference*, Rhodes, Greece, September 2011 (private communication).

Aurass, H., Kurths, J., Mann, G., Chernov, G.P., and Karlicky, M., Estimate of plasma parameters in a coronal loop by means of a fiber burst, *Solar Phys.*, 1987, vol. 108, no. 1, pp. 131–137.

Chernov, G.P., *Fine Structure of Solar Radio Bursts*, Berlin: Springer, 2011.

Chernov, G.P., The relationship between fine structure of the solar radio emission at meter wavelengths and coronal transients, *Astron. Lett.* 1997, vol. 23, no. 6, pp. 827–837.

Chernov, G.P., A comparative analysis of zebra-pattern structures at frequencies from 20 to 7000 MHz, *Astron. Rep.*, 2004, vol. 48, no. 10, pp. 853–870.

Chernov, G.P., Solar radio bursts with drifting stripes in emission and absorption, *Space Sci. Rev.*, 2006, vol. 127, nos. 1–4, pp. 195–326.

Chernov, G.P., Stanislavskii, A.A., Konovalenko, A.A., Abranin, E.P., Dorovsky, V.V., and Rucker, G.O., Fine structure of decametric type II radio bursts, *Astron. Lett.*, 2007, vol. 33, no. 3, pp. 192–202.

Chernov, G.P., Unusual stripes in emission and absorption in solar radio bursts: Ropes of fibers in the meter wave band, *Astron. Lett.*, 2008, vol. 34, no. 7, pp. 486–500.

Kontogeorgos, A., Tsitsipis, P., Caroubalos, C., et al., The improved ARTEMIS IV multichannel solar radio spectrograph of the University of Athens, *Exp. Astron.*, 2006, vol. 21, no. 1, pp. 41–55.

Kruger, A., *Introduction to Solar Radio Astronomy and Radio Physics*, Dordrecht: Reidel, 1979.

Kuijpers, J., Collective wave particle interaction in solar type IV radio sources, *PhD Thesis*, Utrecht: Utrecht Observ., 1975.

Mann, G., Baumgaertel, K., Chernov, G.P., and Karlicky, M., Interpretation of a special fine structure in type IV solar radio bursts, *Solar Phys.*, 1989, vol. 120, no. 2, pp. 383–391.

Slottje, C., *Atlas of Fine Structures of Dynamic Spectra of Solar Type IV-dm and Some Type II Radio Bursts*, Utrecht: Utrecht Observatory, 1981.

Translated by O. Ponomareva